

# Wave Propagation and Diffraction Analysis

Calina Burciu

June 2025

## Abstract

The experiment examined diffraction through single and double slits in Fraunhofer and Fresnel regimes. In Task I, single slit diffraction yielded an average slit width of  $b = 0.172 \text{ mm}$  via manual minima measurement (13.8% error),  $b = 0.217 \text{ mm}$  via curve fitting (8.6% error), and  $b = 0.114 \text{ mm}$  via FFT (42.9% error). Overall, the results support wave optics theory with experimentally reasonable errors.

## 1 Introduction

Diffraction and interference are fundamental principles of wave optics that reveal the wave-like nature of light. When a coherent light source, such as a laser, passes through narrow apertures like slits, it spreads and interferes, producing characteristic intensity patterns. This experiment investigates both single and double slit diffraction in the Fraunhofer and Fresnel regimes, aiming to determine key slit parameters and assess how well experimental results align with theoretical predictions.

## 2 Theoretical Basis

### 2.1 Task 0: Fourier transform of a single slit and a double-slit function

For a single-slit experiment, the slit is modeled by a rectangular function. In the Fraunhofer limit (far-field), the field is described by a Fourier transform of the rectangular function:

$$\Pi(x') = \begin{cases} 1, & -\frac{b}{2} < x' < \frac{b}{2} \\ 0, & \text{else} \end{cases} \quad (1)$$

The spherical waves arriving on the plane of the camera, x-y, is describe by:

$$\Psi(x, y, t) = \int dx' dy' A(x', y') \frac{e^{i(kr - \omega t)}}{r} \quad (2)$$

In the Fraunhofer regime, in the far-field approximation, Eq. 2 transforms to:

$$\Psi(x, y) = \int dx' A_p e^{i(kr - \omega t)} = e^{ik[\sin(\alpha x) + \cos(\alpha x)] - i\omega t} \int dx' A_p e^{-iks \sin(\alpha x')} \quad (3)$$

Calculating the Fast-Fourier-Transform of a  $F(k) = \text{sinc}(2\pi k)$ ,  $F(k) = \text{sinc}^2(2\pi k)$  and  $F(k) = \text{sinc}^2(2\pi k)$  looks like:

$$F(x) = \int_{-\infty}^{\infty} \text{sinc}(2\pi k) e^{-ikx} dk = \frac{1}{2} \Pi\left(\frac{x}{4\pi}\right) \quad (4)$$

$$F(x) = \int_{-\infty}^{\infty} \text{sinc}^2(2\pi k) e^{-ikx} dk = \frac{1}{2} \Lambda\left(\frac{x}{4\pi}\right) \quad (5)$$

So numerically, the FFT of  $\text{sinc}(2\pi k)$  yields a rectangular function in the spatial domain. This mimics the single-slit aperture transmission function. Additionally, it means the FFT of  $\text{sinc}^2(2\pi k)$  will give a triangular function in the spatial domain, wider than the original rect function.

As the amplitude of the waves is depending on the rectangular function, the laser intensity on the camera will be proportional to:

$$I \propto \text{sinc}^2\left(\frac{k_x b}{2}\right) \propto \text{sinc}^2\left(\frac{\pi b \sin \alpha}{\lambda}\right) \quad (6)$$

, for single slit and for double slit

$$I \propto \text{sinc}^2\left(\frac{k_x b}{2}\right) \cos^2\left(\frac{k_x g}{2}\right) \propto \text{sinc}^2\left(\frac{\pi b \sin \alpha}{\lambda}\right) \cos^2\left(\frac{\pi g \sin \alpha}{\lambda}\right) \quad (7)$$

The wave vector  $k_x$  is related by:

$$k_x = \frac{2\pi}{\lambda} \sin \alpha = \frac{2\pi}{\lambda} \frac{x}{\sqrt{x^2 + f^2}} \approx \frac{2\pi x}{\lambda f} \quad (8)$$

The convolution theorem explains that multiplying functions in one domain corresponds to convolving their transforms in the other domain. In the context of Fourier optics, this means that the intensity pattern observed in a diffraction experiment, proportional to the square of the electric field amplitude is the squared magnitude of the Fourier transform of the transmission function. The inverse Fourier transform of this intensity pattern yields the autocorrelation of the slit function. For example, a single rectangular slit has a function  $\text{sinc}$  shaping diffraction amplitude, and its intensity pattern is  $\text{sinc}^2$ . The inverse Fourier transform of this  $\text{sinc}^2$  function gives a triangular function, which is precisely the autocorrelation of the original slit.

Where in a similar sense, the Fourier Solution for equation 7 and utilising the trigonometric identity of  $\cos^2\left(\frac{gk}{2}\right) = \frac{1}{2} + \frac{1}{2} \cos(gk)$ , one can write equation 7 as

$$f(k) = \text{sinc}^2\left(\frac{bk}{2}\right) \left[ \frac{1}{2} + \frac{1}{2} \cos(gk) \right] \quad (9)$$

Applying inverse transforms:

$$\text{sinc}^2\left(\frac{bk}{2}\right) \xleftrightarrow{\mathcal{F}^{-1}} \frac{1}{b} \Lambda\left(\frac{x}{b}\right) \quad (10)$$

$$\frac{1}{2} + \frac{1}{2} \cos(gk) \xleftrightarrow{\mathcal{F}^{-1}} \delta(x) + \frac{1}{2} \delta(x - g) + \frac{1}{2} \delta(x + g) \quad (11)$$

Convolving in real space gives:

$$f(x) = \frac{1}{b} \left[ \Lambda\left(\frac{x}{b}\right) + \frac{1}{2}\Lambda\left(\frac{x-g}{b}\right) + \frac{1}{2}\Lambda\left(\frac{x+g}{b}\right) \right] \quad (12)$$

where  $\Lambda$  behaves in the same manner as a triangle function with;

$$\begin{cases} |x| \leq 1, 1 - x \\ \text{else, } 0 \end{cases} \quad (13)$$

From Fresnel transom, the obtained Fresnel integrals come out (directly taken from the provided guide):

$$F(u) = \int_0^u dx e^{\frac{i\pi x^2}{2}} = C(u) + iS(u) = \int_0^u dx \cos^2\left(\frac{i\pi x^2}{2}\right) + i \int_0^u dx \sin^2\left(\frac{i\pi x^2}{2}\right) \quad (14)$$

Using the Fresnel integrals, the diffraction pattern of a single slit is described by:

$$I \propto \frac{1}{2} \left| F\left(\frac{b+2x}{\sqrt{2\lambda z}}\right) + F\left(\frac{b-2x}{\sqrt{2\lambda z}}\right) \right|^2 \quad (15)$$

For the double slit, the Fresnel diffraction is characterised by:

$$I \propto \frac{1}{2} \left| F\left(\frac{g+b+2x}{\sqrt{2\lambda z}}\right) + F\left(\frac{g+b-2x}{\sqrt{2\lambda z}}\right) - F\left(\frac{g-b+2x}{\sqrt{2\lambda z}}\right) - F\left(\frac{g-b-2x}{\sqrt{2\lambda z}}\right) \right|^2 \quad (16)$$

## 2.2 Theoretical Basis for Single Slit and Double Slit

For the Fraunhofer Configuration, where the approximation of at infinity is realised through the usage of a lens, the positions of minima for an arbitrary order of  $n$  ( $n = \pm 1, \pm 2, \dots$ ) obeys the standard relation for diffraction, as

$$b \sin(\alpha_n) = n\lambda \quad (17)$$

where  $\alpha_n$  corresponds to the deflection angle from the normal of the central intensity spike. Utilising Equation 17, with the relation of intensity and position of minima on the screen, the positions of each minima can be found as

$$x_n = f \cdot \tan(\alpha_n) = f \tan\left[\arcsin\left(\frac{n\lambda}{b}\right)\right] \quad (18)$$

where  $f$  corresponds to the focal length of the lens and  $\lambda$  as the wavelength of the linearly polarised light. Equation 18 can be utilised to find the slit width for a single slit diffraction. Following the same line of thought, the slit distance  $g$  for a double slit configuration of Fraunhofer can be obtained from equation 18, from the relation of angle of deflection for double slit as

$$g \sin(\alpha_n) \approx \left(n + \frac{1}{2}\right)\lambda \rightarrow x_n = f \cdot \tan(\alpha_n) = f \tan\left[\arcsin\left(\frac{(n + \frac{1}{2})\lambda}{g}\right)\right] \quad (19)$$

The slit width,  $b$ , for the double slit can be determined from fitting 7 into the measured intensity profile range.

## 3 Task I: Single Slit

### 3.1 Materials and Set Up

#### 3.1.1 Materials

- Diode laser ( $\lambda = 636 \text{ nm}$ )
- Optical bench
- CCD line camera (Thorlabs)
- Polarizer
- Lens with focal length  $f = 300.8 \text{ mm}$
- Single slit ( $b = 0.2 \text{ mm}$ )
- Residual: PC

#### 3.1.2 Methodology

Setting the CCD camera at a position of 25 mm, the lens at its focal point of  $f = 300.8 \text{ mm}$  from the camera (325.8 mm on the optical bench), and the laser positioned at an arbitrary far enough position, taken to be the far end of the optical bench (refer to Image 1.b). The single slit is positioned at varying positions. For 8 measurements of [325, 675] from the optical bench (absolute distances of [350, 700]), at increments of 50 mm. The said set up relates to the Fraunhofer approximation. At each position the intensity profile is measured and saved.

Using Eq. 8, Eq. 6, and the FFT of the intensity profile, the intensity is plotted as a function of  $k_x$  and the value of  $b$  is determined.

Fresnel Configuration relates to the same set up but without the lens in place. Three measurements were taken, at [200, 350, 650] mm. At each position the intensity profile is measured and saved.

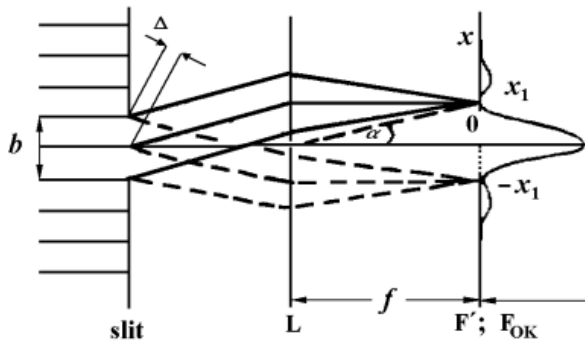


**Image 1.a** Scheme for Task I - Fraunhofer Regime (O17e Diffraction)



**Image 1.b** Setup for Task I - Fraunhofer Regime

### 3.2 Data and Analysis

For task 1(a), the distances  $2x_n$  are measured for each distance from the camera, and the slit width is averaged across the distances. The average  $b_{average, x_n} = 0.17245$  mm for the focal length of  $f = 300.8$  mm, with a relative error of 13.775% from the physical measured value of  $b = 0.2$  mm. It should be noted that, for this part of the analysis, the minima were measured manually, which may have introduced errors that distorted the calculated value of slit width.

$z$ (mm)	$2x_1$ (mm)	$2x_2$ (mm)	$2x_3$ (mm)
325	1.4	3.1	4.4
375	2.9	5.7	8.7
425	1.9	3.8	5.6
475	2.1	3.9	6.0
525	2.3	4.5	7.0
575	2.4	4.8	7.3
625	2.6	5.2	8.1
675	2.9	5.7	8.7

**Table 1:** Distances between minima of each Diffraction Order

In the Fig. 1, it is observed that as the distance from the camera increases, the diffraction pattern becomes wider, whereas at closer distances, the pattern appears narrower. The value at a distance of 375 mm deviates from the overall trend, likely due to a measurement error, as the other data points consistently follow the same pattern.

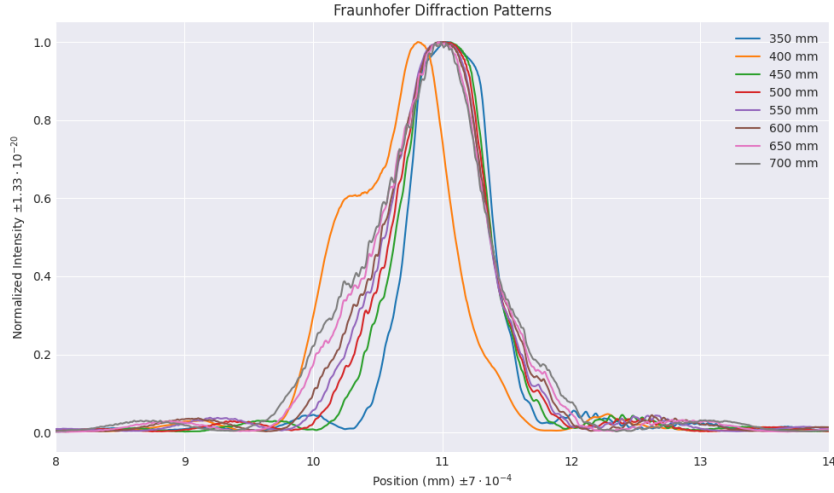


**Figure 1:** Fraunhofer Diffraction Patterns at different Distances from the Camera

For task 1(b), the normalised intensity is plotted as a function of wavevector  $k_x$  for different values of the distance between slit and the camera across the optical bench. The transition between  $x$  and  $k_x$  is done using Eq. 8, after which the Fourier Transform is applied to the intensity profile as a function of the wavevector  $k_x$ . The FFT of the intensity profile corresponds to a triangle shaped function, as theoretically expected in Eq. 5.

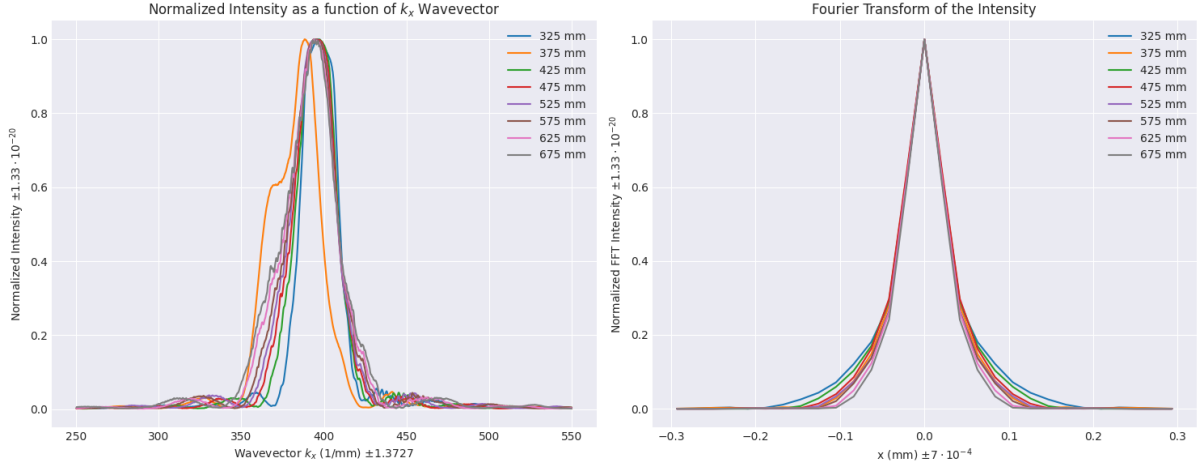


**Figure 2:** Fourier Transform of the Intensity Profile

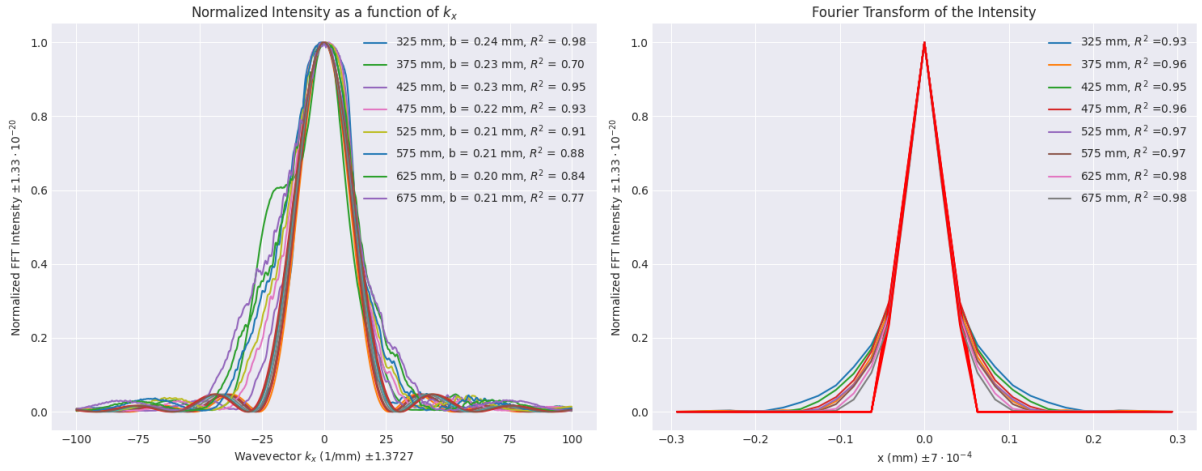


**Figure 3:** Fit Curves of the Intensity Profile & Fourier Transform of the Intensity

In the same task, it is necessary to find the slit width using a fit of the Eq. 14 and additionally from the Fourier transform of the intensity profile. The fitted values were found for each of the distances, with an average value of  $b_{average,k_n} = 0.21717mm$  and corresponding to  $r^2$  scores between  $r^2_{d=325mm} = 0.98$  and  $r^2_{d=375mm} = 0.70$ , as seen in first graph of Fig. 3. The average slit width from the fitted values of the Fourier transform of intensity is  $b_{average,k_n} = 0.1143mm$ , with really good  $r^2$  scores, but with a 42,85% relative error from the measured value of the slit.

For task 1(c), in the Fresnel regime, Eq.16 is used to compare the patterns. In Fig. 4, the sum of Fresnel integrals is used to compare the intensity profile captured in the Fresnel regime. The function plotted additionally corresponds to the theoretical Fresnel integrals with the  $b$  width slit found from the task 1(a).

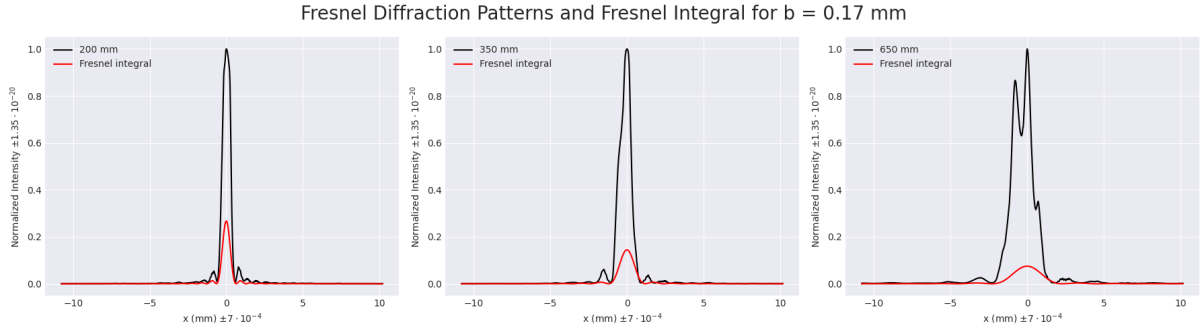


**Figure 4:** Fresnel Diffraction Pattern

### 3.3 Discussion

In the single-slit experiment, the results are consistent with theoretical predictions. Using a lens helps the formation of the Fraunhofer diffraction pattern at its focal plane, allowing clear observation of the diffraction features even at short distances. At greater distances with or without a lens, the pattern typically becomes broader, but it may suffer from noise due to medium factors. The lens helps produce smoother and more stable intensity profiles at closer ranges, offering a cleaner view of the diffraction envelope.

Overall, the observed widening of the diffraction pattern with increasing distance aligns with the expected behaviour of single-slit Fraunhofer diffraction. The diffraction angles are fixed for a given wavelength and slit width. However, as the camera is farther from the slit, these constant angles correspond to the increasing linear distances on the screen. So even though the angular pattern doesn't change, the physical spread of the pattern appears to widen with distance.

The transformation from spatial position to wavevector  $k_x$ , in task 2(b), is performed smoothly and doesn't significantly change the overall intensity trend. The Fourier transform of the intensity as a function of  $k_x$  shows a result comparable with a triangular shaped function. This is most visible at larger distances, which better approximate the Fraunhofer diffraction regime, while at the smaller distances, the profile becomes more curved near the base. While not a perfect triangle, the symmetry and peak structure agree with the diffraction pattern for a single slit.

In this context, when analysing diffraction patterns, deviations from ideal shapes often arise due to practical experimental conditions. For smaller values, such as 325 mm, a curve appears at the base of the graph. This is because, at these distances, the light spreads over a larger surface and is not yet concentrated into a single spot, leading to observable distortions in the expected pattern.

To determine the slit width  $b$ , the intensity data were fitted using Eq. 6 and the resulting values of  $b$  were averaged. The final average value,  $b_{average, k_n}$ , has a relative error of 8,58% compared to the physically measured slit width. This indicates good agreement with the theoretical model, supported by high values of  $r^2$  scores.

In the fitting of the Fourier transform of the intensity, the  $b$  slit width is found with good  $r^2$  scores, but values of the width way off from the real value of  $b$ . With a relative error of 42,85%, this method shows a bad correlation between the theoretical expectations and the actual data. The discrepancy likely arises from the method's sensitivity to noise, limited resolution, and imperfections in the recorded intensity profile, all of which can distort the Fourier transformed signal and lead to inaccurate fitting.

Among the three methods for determining the slit width  $b$ , the direct fitting of the

intensity profile as a function of  $k_x$  using the theoretical  $\text{sinc}^2$  model (Eq. 6) shows the most accurate results, with a relative error of only 8.58% and high  $r^2$  scores, indicating strong agreement with theory.

In the attempt to compare the Fresnel diffraction pattern using the Fresnel functions on intensity profile, three distances were analysed. However, same in this case, the functions don't accurately describe the observed trends as one of the intensity profile even shows two distinct peaks and deviates from the expected shape.

This difference reflects the complexity of the Fresnel regime. Unlike the Fraunhofer regime, where diffraction patterns are well-defined and predictable, Fresnel diffraction often leads to less symmetric intensity distributions, especially when the observation screen is relatively far from the slit. The transition from near-field (Fresnel) to far-field (Fraunhofer) is gradual, as the pattern may display characteristics of both, making it difficult to model using simple analytical functions.

Another factor that may have contributed to measurement inaccuracies in the Fresnel regime is the insufficient use of the polarizer, which resulted in too high intensity levels. This likely effect the accurate detection of the diffraction trend, as the detector may have become saturated or overwhelmed, masking finer details in the pattern.

### 3.4 Error Analysis

The uncertainty in intensity and position is the smallest measurable increment from the digital device. Where the normalised intensity is derived through standard relation between parameters with uncertainty. And the values of  $b$  and  $g$  through standard deviation (as they are found through either linear regression or a fit). The uncertainty in the found values  $k_x$  are found by propagating the measured values through their respective square root of partial derivatives of all input values and taking the mean, as follows:

$$\Delta k_x = \sqrt{\left(\frac{\partial k_x}{\partial x} \Delta x\right)^2 + \left(\frac{\partial k_x}{\partial f} \Delta f\right)^2} \quad (20)$$

$$\Delta b = \sqrt{\frac{1}{N-1} \sum_{i=1}^N (b_i - \bar{b})^2} \quad (21)$$

$$\Delta I_{\text{Fraun} / \text{Fresn, Normalised}} = \left( \frac{\Delta I_{\text{Fraun} / \text{Fresn}}}{I_{\text{Fraun} / \text{Fresn}}} + \frac{\Delta I_{\text{Fraun} / \text{Fresn, max}}}{I_{\text{Fraun} / \text{Fresnmax}}} \right) \cdot I_{\text{Fraun} / \text{Fresn, Normalised}} \quad (22)$$

Parameter	Mean	Maximum
$\Delta k_x (mm^{-1})$	$\approx 1.37$	$\approx 2.74$
$\Delta x_d (mm)$	$1.7 \cdot 10^{-6}$	-
$\Delta b_{x_n} (mm)$	$\approx 4.45 \cdot 10^{-5}$	$\approx 4.45 \cdot 10^{-5}$
$\Delta I_{\text{Fraunhofer, Normalised}}$ (no units)	$\approx 1.33 \cdot 10^{-20}$	$\approx 2.61 \cdot 10^{-20}$
$\Delta I_{\text{Fresnel, Normalised}}$ (no units)	$\approx 1.32 \cdot 10^{-20}$	$\approx 2.66 \cdot 10^{-20}$

**Table 2:** Mean and Maximum Uncertainty Parameters of Task 1



## 4 Conclusion

Overall the experiment was successful, where there were the expected result in the diffraction spectrum. However, due to some systematic issues, there is a prominent level of deviation from the expected results, and presents an issue with our experimental procedure. Future experimental exploration will be redoing the experiment with more precision and care, to ensure least deviation possible. Additional experiments will be looking into diffracting grating, with large amounts of slits, testing the Fraunhofer at a much larger distance and approximating Fresnel through fitting. This would make it a good comparison between the two methods.